

Proteolytic Activation of Rim1p, a Positive Regulator of Yeast Sporulation and Invasive Growth

Weishi Li and Aaron P. Mitchell

Department of Microbiology and Institute of Cancer Research, Columbia University, New York, New York 10032

Manuscript received March 1, 1996
Accepted for publication October 4, 1996

ABSTRACT

In the yeast *Saccharomyces cerevisiae*, *rim1*, *8*, *9*, or *13* mutations cause four phenotypes: poor growth at low temperature, altered colony morphology, inefficient sporulation due to reduced expression of the meiotic activator *IME1*, and, as shown here, defective invasive growth. In this report, we have determined the relationship between *RIM1* and the other genes, *RIM8*, *9*, and *13*, in this group. We have analyzed production of epitope-tagged Rim1p derivatives with HA epitopes at the N-terminus or in the middle of the protein. These Rim1p derivatives exist primarily as a small form (90 kD for Rim1-HA2p) in wild-type cells and as a large form (98 kD for Rim1-HA2p) in *rim8*, *9*, and *13* mutants. We have also analyzed production of β -galactosidase in strains that express a *RIM1-lacZ* fusion gene. β -galactosidase exists primarily as a \sim 130 kD form in wild-type cells and as a \sim 190 kD form in *rim9* mutants. These results indicate that Rim1p undergoes C-terminal proteolytic cleavage, and that *rim8*, *9*, and *13* mutations block cleavage. Expression of a Rim1p C-terminal deletion derivative suppresses *rim8*, *9*, and *13* mutations. Thus the phenotypes of *rim8*, *9*, and *13* mutants arise from the defect in Rim1p C-terminal cleavage. Cleavage of Rim1p, like that of its *Aspergillus nidulans* homologue PacC, is stimulated under alkaline growth conditions. Therefore, Rim1p, PacC and their respective processing pathways may represent a conserved signal transduction pathway.

ENTRY of yeast cells into meiosis is restricted to one kind of cell, the *a*/ α cell, and occurs only under poor nutritional conditions (reviewed in MILLER 1989). These conditions include absence of a fermentable carbon source, such as glucose, and limitation for nitrogen or other nutrients. The meiotic program is initiated with increased accumulation of the *IME1* transcript; the *IME1* gene product activates expression of a large number of early meiotic genes (reviewed by MITCHELL 1994).

The mechanisms by which the cell senses and responds to nutrient limitation are unclear. One approach to this problem has been to identify genes that govern *IME1* expression. Positive regulators of *IME1* lie in three pathways (NEIGEBORN and MITCHELL 1991; SHAH and CLANCY 1992; SU and MITCHELL 1993a,b). One pathway includes *IME4*, which is expressed at highest levels in nitrogen-starved *a*/ α cells (SHAH and CLANCY 1992). A second pathway includes *MCK1*, which specifies a serine/threonine/tyrosine-protein kinase (DAILEY *et al.* 1990; NEIGEBORN and MITCHELL 1991; SHERO and HIETER 1991). The third pathway includes four genes: *RIM1*, *RIM8*, *RIM9*, and *RIM13*. Recessive mutations in these *RIM* genes cause reduced *IME1* expression, cold-sensitive growth, and altered colony mor-

phology (SU and MITCHELL 1993a). The similarity of *rim1*, *8*, *9*, and *13* mutant phenotypes has led to the inference that these *RIM* gene products have related physiological functions. Analysis of double mutants has suggested that Rim1p, 8p, 9p, and 13p act in a distinct pathway from Mck1p and Ime4p: *rim mck1* and *rim ime4* double mutants have more severe sporulation defects than any of the single mutants, whereas *rim rim* double mutants have defects similar to *rim* single mutants (SU and MITCHELL 1993a,b). Therefore, the *RIM* gene products may act together in a protein complex or in successive steps of a linear pathway.

RIM1 specifies a 628 residue protein with three C₂H₂ zinc fingers and a C-terminal acidic region. TILBURN *et al.* (1995) have recently reported that the *Aspergillus* PacC protein is homologous to Rim1p over the zinc-finger region. Both proteins are also of similar size and have acidic C-terminal regions. These findings raise the possibility that Rim1p and PacC may act in a conserved pathway. PacC is a downstream component in a pH-response pathway, as indicated by four main observations. First, loss-of-function *pacC* defects prevent alkaline responses, as do mutations in other *pal* genes (TILBURN *et al.* 1995). Second, activating *pacC^C* mutations promote alkaline responses in acid-grown cells. Third, several *pal* mutations are suppressed by *pacC^C* mutations. Fourth, PacC is activated by C-terminal proteolytic cleavage in alkaline-grown cells, and several *pal* mutants are defective in PacC cleavage (OREJAS *et al.*

Corresponding author: Aaron Mitchell, Institute of Cancer Research, Columbia University, 701 West 168th St., New York, NY 10032.
E-mail: apm4@columbia.edu

1995). Functional importance of PacC cleavage is supported by the finding that *pacC^c* alleles encode C-terminal PacC truncation derivatives. We report here evidence that Rim1p is activated through a similar regulatory pathway.

MATERIALS AND METHODS

Strains and media: All *Saccharomyces cerevisiae* strains are derivatives of SK-1 (KANE and ROTH 1974) and are listed in Table 1. Mutations previously described include *ura3*, *leu2::hisG*, *trp1::hisG*, *lys2*, *ho::LYS2* (ALANI *et al.* 1987), *rme1Δ5::LEU2* (COVITZ *et al.* 1991), *ime2-4-lacZ::LEU2*, *ime1-13::HIS3* (NEIGEBORN and MITCHELL 1991), *IME2-5-lacZ-URA3*, *rim1-1*, *rim8-1*, *rim9-1*, *rim13-1*, *met4*, *arg6* (SU and MITCHELL 1993a), and *rim1Δ5::URA3* (SU and MITCHELL 1993b). Mutations in *RIM1* and *RIM9* that were constructed in this study are listed separately below. Standard recipes were used for SD, SC, SC dropout media, 5-FOA plates, YPD, YPac, KAc-Xgal, sporulation plates, and liquid sporulation medium (SMITH and MITCHELL 1989; SU and MITCHELL 1993a; KAISER *et al.* 1994). Media were buffered, where noted in RESULTS, with 100 mM sodium phosphate at the indicated pH. Yeast strains were routinely grown at 30°. Standard procedures were used for mating, diploid selection, tetrad analysis, and PCR genotype determinations (KAISER *et al.* 1994).

rim mutant phenotypic tests: *rim* mutations were routinely followed in crosses through two phenotypic tests. First, colony morphology was determined by visual inspection. *rim1*, *8*, *9*, and *13* mutants have a smooth colony morphology, whereas *RIM* strains have a rough colony morphology in the SK-1 genetic background (SU and MITCHELL 1993a). Second, complementation of *rim* mutant testers was determined through *ime2-lacZ* expression assays. Segregants were mated to **a** and **α** *rim ime2-lacZ* strains, diploids were selected on counterselective medium (generally SD +Lys), and *ime2-lacZ* expression was determined after incubation of diploids for 3 days on KAc-Xgal plates (SU and MITCHELL 1993a). Under these conditions, *rim/rim* diploid patches remain white and *RIM/rim* diploid patches turn blue. The testers were strains AMP1585 and AMP1586 (*rim8*), AMP1587 and AMP1588 (*rim9*), and AMP1589 and AMP1590 (*rim13*). *ime2-lacZ* expression was also monitored in haploid **a** and **α** strains that carry a *rme1Δ5* mutation (SU and MITCHELL 1993a), which relieves cell-type control over meiosis and meiotic gene expression (reviewed by MITCHELL 1994).

To score *ime1-HIS3* expression, strains carrying a chromosomal *ime1-HIS3* fusion gene (NEIGEBORN and MITCHELL 1991) were grown as patches on medium containing histidine, then replica-plated lightly to SC –His and control SC plates. Growth was scored after 2 days. *rim1*, *8*, *9*, and *13* mutants fail to grow on the SC –His plate under these conditions. We note that this growth test is independent of *RME1* or cell-type control (NEIGEBORN and MITCHELL 1991), presumably because it monitors basal *IME1* promoter activity.

To score cold-sensitive growth, strains were streaked for single colonies on a YPD plate and incubated at 17° for 7 days. *rim1*, *8*, *9*, and *13* mutants form much smaller colonies than wild-type strains under these conditions.

To score invasive growth, strains were grown as patches on YPD plates for 1 day at 30° and for 2 more days at room temperature. Cells were washed from the surface of the plate under water (BLACKETER *et al.* 1993) while agitating cells with a spreader. This procedure permitted visualization of cells that had penetrated the surface of the agar. *rim1*, *8*, *9*, and *13* mutants fail to penetrate the agar surface.

***RIM1-7::URA3* mutation:** This allele introduces a *URA3* marker linked to a functional *RIM1* allele, through integration of plasmid pSS253. This plasmid was constructed by ligation of a 0.55-kb *PstI*-*BglII* fragment, including *RIM1* sequences from –531 to codon 6, into plasmid YIp356R (MYERS *et al.* 1986) digested with *PstI* and *Bam*HI. Integration at *RIM1* was confirmed by Southern analysis.

***rim1Δ12* mutation:** This unmarked deletion removes *RIM1* codons 7–628 and 800 bp of 3' sequences. The *rim1Δ12* integrative plasmid pWL28 was constructed as follows. A 2.8-kb *BglII* fragment that includes the *RIM1* gene was deleted from plasmid pSS179*RIM1* (SU and MITCHELL 1993b) to generate plasmid pWL27. The deletion and flanking sequences were then moved as a 3.5-kb *Sall*-*KpnI* fragment from pWL27 to integrating plasmid pRS306 (SIKORSKI and HIETER 1989) to create pWL28. A *RIM1* strain (KB38) was transformed with a *XhoI* digest of pWL28, and *Ura⁺* transformants were streaked on 5-FOA plates to select for loss of the *URA3* marker. Presence of *rim1Δ12* was confirmed by *rim1* complementation tests and Southern analysis.

Epitope-tagged *RIM1-HA* alleles: Multi-copy plasmids specifying hemagglutinin (HA) epitope-tagged *RIM1* alleles were constructed from plasmid pWL32, a derivative of multi-copy *RIM1* plasmid pMCRIM1 (SU and MITCHELL 1993b) in which the vector *NotI* site was destroyed. pWL32 was subjected to site-directed mutagenesis to create unique *NotI* sites following *RIM1* codon 1 (plasmid pWL33), codon 312 (pWL34), codon 473 (pWL35), or codon 613 (pWL36). A *NotI* fragment from the GTEP plasmid (TYERS *et al.* 1993), encoding three HA epitopes, was inserted into *NotI* sites of pWL33, pWL34, pWL35, and pWL36 to create pWL39 (*RIM1-HA1*), pWL40 (*RIM1-HA2*), pWL41 (*RIM1-HA3*), and pWL42 (*RIM1-HA4*), respectively. Insertions and junction sites were verified by sequencing. This analysis revealed that pWL40 carried three head-to-tail insertions of the GTEP fragment, specifying nine HA epitopes. The other plasmids carried single GTEP fragment insertions. Each multi-copy *RIM1-HA* plasmid could complement a *rim1* mutant strain.

RIM1-HA alleles were introduced into the genomic *RIM1* locus through cotransformation with 1 μg of *TRP1* plasmid pRS314 (SIKORSKI and HIETER 1989) and 5 μg of Asp718/*Sall* digests of *RIM1-HA* plasmids and into strain W1057 (*trp1 rim1Δ12 ime2-lacZ*). *Trp⁺* transformants were screened for acquisition of *Rim⁺* phenotypes (expression of *ime2-lacZ* and formation of rough colonies) and appeared at a frequency of 1%. Presence of *RIM1-HA* alleles was confirmed by Southern analysis.

rim8, *rim9*, and *rim13* mutant strains carrying epitope-tagged *RIM1-HA2* (strains AMP1582, AMP1584, and AMP1583) were identified among meiotic segregants of crosses between AMP1611 (*RIM1-HA2*) and AMP1579 (*rim8-1*), AMP1580 (*rim9-1*), and AMP1581 (*rim13-1*). PCR analysis distinguished *RIM1-HA2* (1.3-kb product) from *RIM1* (1.0-kb product) with primers *RIM1*-PKA2 (5'-CAAAAAGAAGCTTCTAAGAAAAAC-3', hybridizing to *RIM1* codons 251–258) and *RIM1*-KNP6 (5'-CCCAACATCTCTACG-3', hybridizing to *RIM1* codons 567–562). *rim8*, *rim9*, and *rim13* mutant strains carrying *RIM1-HA2-531* (strains AMP1597, AMP1598, and AMP1599) were identified among meiotic segregants of crosses between AMP1593 (*RIM1-HA2-531*) and AMP1574 (*rim8-1*), AMP1595 (*RIM1-HA2-531*) and AMP1596 (*rim9-10*), and AMP1595 (*RIM1-HA2-531*) and AMP1576 (*rim13-1*). *RIM1-HA2-531* was followed through the associated *TRP1* marker. Smooth and rough colony morphology segregated as a two-gene trait (two smooth:two rough, one smooth:three rough, and zero smooth:four rough tetrads). *rim RIM1-HA2-531* were deduced to be the two *Trp⁺* segregants in NPD (zero smooth:four rough) tetrads. Presence

TABLE 1
Yeast strains

Strain	Genotype ^a	Source
AMP107	a <i>RME1 IME2</i>	This lab
AMP109	a/α <i>RME1/RME1 IME2/IME2</i>	This lab
AMP1571	a <i>his3 arg6 RME1 IME2</i>	This study
AMP1572	α <i>arg6</i>	This lab
AMP1573	α <i>met4 rim9-1</i>	This lab
AMP1574	a <i>rim8-1 arg6</i>	This study
AMP1575	α <i>met4 rim8-1</i>	This lab
AMP1576	α <i>rim13-1 arg6 met4</i>	This lab
AMP1577	a/α <i>rim9-1/rim9-1 IME1/ime1-HIS3 met4/MET4 ime2-4-lacZ::LEU2/IME2 his3/his3 ARG6/arg6</i>	This lab
AMP1578	a/α <i>rim1Δ1::URA3/rim1Δ1::URA3 ime1-HIS3/IME1 rme1Δ5::LEU2/RME1 his3/his3 arg6/ARG6 IME2-5-lacZ::URA3/IME2</i>	SU and MITCHELL (1993b)
AMP1579	a <i>RIM1-7::URA3 rim8-1 his3 RME1 IME2</i>	This study
AMP1580	a <i>RIM1-7::URA3 rim9-1 RME1 IME2</i>	This study
AMP1581	a <i>RIM1-7::URA3 rim13-1 his4 arg6 met4 RME1 IME2</i>	This study
AMP1582	α <i>RIM1-HA2 rim8-1 arg6 met4 IME2</i>	This study
AMP1583	α <i>RIM1-HA2 rim13-1 his4 IME2</i>	This study
AMP1584	α <i>RIM1-HA2 rim9-1 IME2</i>	This study
AMP1585	a <i>rim8-1 his1 gal80::LEU2</i>	This study
AMP1586	α <i>rim8-1 his1 gal80::LEU2 RME1</i>	This study
AMP1587	a <i>rim9-1 his1 gal80::LEU2 RME1</i>	This study
AMP1588	α <i>rim9-1 his1 gal80::LEU2</i>	This study
AMP1589	a <i>rim13-1 his1</i>	This study
AMP1590	α <i>rim13-1 his1 gal80::LEU2 RME1</i>	This study
AMP1591	α <i>RIM1-HA2 IME2</i>	This study
AMP1592	a/α <i>rim9Δ2/rim9Δ2 RME1/RME1 arg6/ARG6 ime1-HIS3/IME1 IME2-5-lacZ::URA3/IME2 his3/his3</i>	This study
AMP1593	α <i>RIM1-HA2-531 IME2</i>	This study
AMP1594	a/α <i>rim9-10::URA3/RIM9 RME1/RME1 IME2/IME2</i>	This study
AMP1595	a <i>RIM1-HA2-531</i>	This study
AMP1596	α <i>rim9-10::URA3 arg6</i>	This study
AMP1597	α <i>RIM1-531::TRP1 rim8-1 arg6</i>	This study
AMP1598	α <i>RIM1-531::TRP1 rim9-10::URA3 arg6</i>	This study
AMP1599	α <i>RIM1-531::TRP1 rim13-1 met4</i>	This study
AMP1600	α <i>RIM1-531::TRP1</i>	This study
AMP1601	α <i>RIM1-HA2 rim9-10::URA3 arg6</i>	This study
AMP1602	α <i>RIM1-HA2 rim8-1 arg6</i>	This study
AMP1603	α <i>RIM1-HA2 rim13-1 arg6</i>	This study
AMP1604	α <i>RIM1-HA2 arg6</i>	This study
AMP1605	α <i>rim1Δ12 arg6</i>	This study
AMP1606	α <i>arg6 his3</i>	This study
AMP1607	a <i>rim1-1 IME2</i>	This study
AMP1608	α <i>RIM1-HA1 arg6</i>	This study
AMP1609	α <i>RIM1-HA2 arg6</i>	This study
AMP1610	α <i>RIM1-HA3 arg6</i>	This study
AMP1611	α <i>RIM1-HA2 arg6 IME2</i>	This study
AMP1686	α <i>RIM1-13-lacZ::URA3 IME2</i>	This study
AMP1687	a <i>rim9-10::URA3 arg6 IME2</i>	This study
AMP1688	a <i>rim9-10::URA3 RIM1-13-lacZ::URA3 IME2</i>	This study

^a All strains have the additional markers *rme1Δ5::LEU2*, *IME2-5-lacZ::URA3*, *ura3*, *leu2::hisG*, *trp1::hisG*, *lys2* and *ho::LYS2*, unless otherwise indicated.

of *rim* mutations in strains AMP1597, AMP1598, and AMP1599 was verified in meiotic analysis of crosses to a wild-type strain (AMP107) by recovery of segregants forming smooth colonies. Suppression of each *rim* mutation by *RIM1-HA2-531* was confirmed by meiotic analysis of crosses to respective *rim* testers, yielding two smooth Trp⁻:2 rough Trp⁺ segregation.

RIM1-HA2 was expressed in *Escherichia coli* (STUDIER *et al.*

1990) from plasmid pWL83, in which *RIM1-HA2* on a *BglII-EcoRV* fragment from pWL40 was inserted between the *BamHI* and *EcoRV* sites of pET-3b (Pharmacia). This construct fuses *RIM1-HA2* at codon 6 to a 12-codon leader. Bacterially produced Rim1-HA2p was identified by comparison of extracts from induced and uninduced cells.

***RIM1-lacZ* fusion:** The *RIM1-lacZ* fusion plasmid pWL142

was constructed by insertion of *Bgl*II-*Bam*HI fragment from plasmid pWL42 into the *Bam*HI site of *lacZ URA3* plasmid Yip356R (MYERS *et al.* 1986). This insert carries codons 6–613 of *RIM1* and a portion of the triple HA epitope from the *RIM1-HA4* allele. pWL42 was digested with *Xmn*I, and singly cut partial digestion products were gel purified for integrative transformation. (*Xmn*I cuts once in *RIM1* sequences and once in the vector.) Ura⁺ transformants were selected, and integration at *RIM1* was confirmed by Southern analysis. The genetic designation for these transformants, *RIM1-13-lacZ::URA3*, is abbreviated as *RIM1-lacZ* in the text of this paper. The transformant AMP1686 (α *RIM1-lacZ*) was crossed to strain AMP1687 (*a rim9-10*) to obtain meiotic *RIM1-lacZ rim9-10* segregant AMP1688.

***RIM1* 3' deletion derivatives:** *RIM1* deletion derivatives on plasmids pKN30, 32, 34, 35, 36, and 39 were generated through exonuclease III digestion (Promega) of plasmid pSS179*RIM1* (SU and MITCHELL 1993b). Endpoints were determined by sequence analysis. In the course of these studies, we found that the pKN34 deletion endpoint to be codon 539, not codon 531 as reported (SU and MITCHELL 1993b). The *RIM1-531* plasmids pWL86 and pWL88 were constructed by inserting a 2.1-kb *Pst*I-*Xho*I fragment from plasmid pSS239-CRX (SU and MITCHELL 1993b) between the *Pst*I and *Xho*I sites of pRS314 and pRS304 (SIKORSKI and HIETER 1989), respectively. Resulting plasmids include *RIM1* 5' sequences and coding region through codon 531; the fusion to vector sequences adds C-terminal amino acids RILLEGPGTSCSL.

The chromosomal *RIM1-HA2-531* allele was created as follows. *RIM1-531* plasmid pWL88 was cleaved at a unique *Spy*I site within *RIM1* and transformed into strain AMP1591 (*RIM1-HA2*); cleavage was expected to promote insertion 3' of the *RIM1-HA2* epitope site in the genome. Transformant strain AMP1593 had the expected structure from pWL88 integration: one copy of a *RIM1-HA2* derivative that terminates at codon 531 followed by pRS304 vector sequences and one copy of wild-type *RIM1*. The genotype was confirmed by PCR analysis using primer *RIM1*-PKA2 (5'-CAAAAAGAAGCTTCTA-AGAAAAAC-3') and an M13 reverse primer (Stratagene). Integration at the *RIM1* locus was confirmed by meiotic segregation (eight parental ditype tetrads) from a cross of strain AMP1593 to a *rim1 Δ 5::URA3* strain.

Cloning of *RIM9*: Diploid strain AMP1577 (*rim9-1/rim9-1 +/ime1-HIS3 ime2-lacZ/+*) was transformed with genomic libraries carried in YCp50 (ROSE *et al.* 1987), a low copy number *URA3*-bearing plasmid. Transformants were patched on SC –Ura plates, then replica-plated to KAc-Xgal plates for scoring *ime2-lacZ* expression, and SC –His plates for scoring *ime1-HIS3* expression. Purified Lac⁺ His⁺ transformants were checked for plasmid linkage of Ura⁺, Lac⁺, and His⁺ phenotypes by cocuring and by transformation of isolated plasmids into strain AMP1577. A 3-kb *Eco*RI fragment from one complementing plasmid (pWL51) was inserted into YIp5 *Eco*RI site to create integrating plasmid pWL48. pWL48 was transformed into a wild-type *RIM9* strain after *Bgl*II cleavage within the insert. The transformant was crossed to a *rim9-1* strain and 24 meiotic tetrads analyzed indicated tight linkage between *RIM9* and the plasmid *URA3* marker (23 PD, 0N, 1 T).

***RIM9* sequence determination:** Initial sequence and subclone analysis indicated that *RIM9* lies between the *NCA1* gene (PAYNE *et al.* 1993; ZIAJA *et al.* 1993) and a putative *ARG7* gene (W. LI and A. P. MITCHELL, unpublished observations). A 1.5-kb *Asp*718-*Nsi*I fragment spanning this region was sequenced with complementary oligonucleotides derived from sequence information in GENBANK.

***rim9 Δ 2* mutation:** This deletion removes *RIM9* codons 1–71 (of the 239 codon open reading frame), *RIM9* 5' se-

quences, and part of the adjacent *ARG7* gene. The deletion was created in plasmid pWL76, which has a 5-kb *Kpn*I-*Eco*RI fragment carrying *RIM9* in the integrating *URA3* vector pRS306 (SIKORSKI and HIETER 1989). The *rim9 Δ 2* plasmid pWL85 resulted from deletion of a *Sal*I fragment from pWL76. Plasmid pWL85 was cleaved at a unique *Sph*I site and transformed into haploid strain AMP107. Ura⁺ transformants were then streaked on 5-FOA plates to select for loss of the *URA3* marker. A Ura[–] segregant that displayed smooth colony morphology and cold-sensitive growth was confirmed to carry *rim9 Δ 2* by Southern analysis. Growth tests confirmed that *rim9 Δ 2* also causes an arginine requirement.

***rim9-10::URA3* mutation:** This mutation is an insertion of *URA3* into *RIM9* at codon 12. The insertion was created in plasmid pWL62, which has a 2.3-kb *Sal*I fragment carrying *RIM9* in vector pRS314 (SIKORSKI and HIETER 1989). The *rim9-10::URA3* plasmid pWL104 resulted from ligation of *URA3*, within a 1.1-kb *Sma*I fragment from pSM14-6 (provided by SUSAN MICHAELIS), into a filled-in *Nhe*I site in plasmid pWL62. A *Hind*III digest of pWL104 was transformed into diploid strain AMP109, and presence of *rim9-10::URA3* was verified among Ura⁺ transformants by Southern. All 26 meiotic tetrads from transformant AMP1594 (*RIM9/rim9-10::URA3*) displayed two smooth Ura⁺:two rough Ura[–] segregation. Subsequent studies indicated that this mutation causes the same defects in invasive growth, low-temperature growth, colony morphology, *ime1-HIS3* expression, *ime2-lacZ* expression, and sporulation as the original *rim9-1* mutation (SU and MITCHELL 1993a; data not shown).

Immunoblots: Cells from 1 ml of exponential phase culture were pelleted, resuspended in 30 μ l Laemmli buffer, boiled for 5 min, and fractionated on a 7% SDS-polyacrylamide gel. Proteins were transferred to a nitrocellulose filter, which was probed with anti-HA monoclonal ascites fluid (12CA5 monoclonal; Babco; 10^{–4} dilution) or anti- β -galactosidase monoclonal antibody (Promega; 0.5 \times 10^{–3} dilution) and goat anti-mouse IgG conjugated to peroxidase (Boehringer Mannheim; 10^{–4} dilution), following standard methods (BOWDISH *et al.* 1994). The immunoblot was developed with ECL detection reagents (Amersham), following the manufacturer's instructions.

β -galactosidase assays: Plate assays were conducted on KAc-Xgal plates as previously described (SU and MITCHELL 1993a). Quantitative β -galactosidase assays were performed on permeabilized cells as previously described (SMITH *et al.* 1990). Cells were shifted from exponential phase in YPac to sporulation medium for 8 hr before assays. All numbers reported are mean averages of determinations with three cultures.

RESULTS

Dependence of haploid invasive growth on *RIM* gene function: Mutations in the genes *RIM1*, *RIM8*, *RIM9*, and *RIM13* cause a common set of phenotypes, including reduced expression of the meiotic activator, *IME1* (resulting in reduced meiotic gene expression and sporulation ability), poor growth at low temperatures, and smooth colony morphology in the otherwise rough SK-1 strain background (SU and MITCHELL 1993a). GIMENO *et al.* (1992) showed that certain *S. cerevisiae* strains with smooth colony morphology are defective in production of aerial pseudohyphae during nitrogen limitation of α/α cells (GIMENO *et al.* 1992). However, we observed

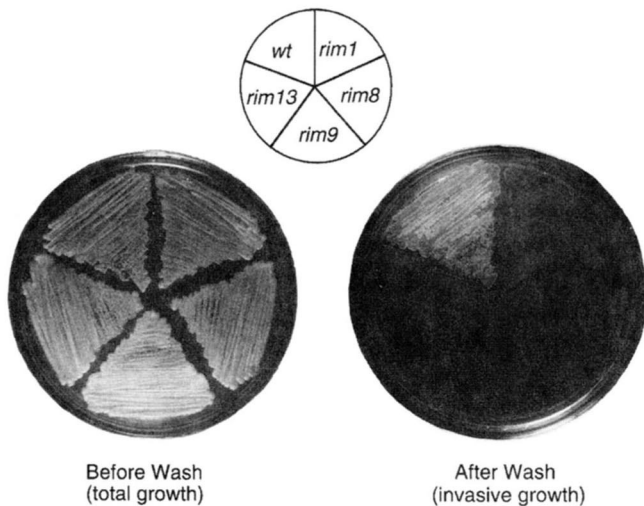


FIGURE 1.—Effects of *rim1*, *8*, *9*, and *13* mutations on haploid invasive growth. Haploid strains grown as patches on a YPD plate as described in MATERIALS AND METHODS. Plates were photographed before (total growth) and after (invasive growth) washing the cells from the agar surface. Strains were AMP1572 (*RIM*), AMP1605 (*rim1* Δ 12), AMP1575 (*rim8-1*), AMP1573 (*rim9-1*), and AMP1576 (*rim13-1*).

no defect in pseudohyphal growth of \mathbf{a}/α *rim/rim* mutant strains (data not shown). \mathbf{a} and α cells can produce chains of cells, similar to pseudohyphae, that invade an agar growth substrate (BLACKETER *et al.* 1993; ROBERTS and FINK 1995). The signal that promotes invasive growth is unknown. We found that *rim1-1*, *8-1*, *9-1*, and *13-1* mutations prevent invasive growth of haploid \mathbf{a} and α cells (Figure 1). The *rim1* Δ 12, *rim9-2* and *rim9* Δ 10 mutations, which also prevent invasive growth (data not shown), must cause a loss of gene function, based upon their structural features (see MATERIALS AND METHODS). The *rim8-1* and *rim13-1* mutations are recessive, based upon sporulation, colony morphology, and low temperature growth (SU and MITCHELL 1993a), and thus are likely to reduce or abolish gene function. We conclude that Rim1p, Rim9p, and (probably) Rim8p and Rim13p are formally positive regulators of haploid invasive growth.

Effects of *rim8*, *9*, and *13* mutations on Rim1p: To monitor accumulation of Rim1p polypeptide, we introduced HA insertions into three hydrophilic regions. A cassette specifying HA epitopes (TYERS *et al.* 1993) was inserted after *RIM1* codon 1 (*RIM1-HA1*), codon 312 (*RIM1-HA2*), or codon 478 (*RIM1-HA3*). Sequence determination revealed that *RIM1-HA1* and *RIM1-HA3* each had a single epitope cassette, whereas *RIM1-HA2* had three consecutive epitope cassettes. Analysis of multi-copy plasmid-borne *RIM1-HA* alleles indicated that they retained significant function (data not shown). We quantitated activity of each allele after insertion at the genomic *RIM1* locus through assays of *ime2-lacZ* expression and sporulation (Figure 2). *ime2-*

lacZ assays were conducted on haploid *rme1* strains; sporulation was assayed in *RIM1-HA/rim1-1* diploids. *RIM1-HA2*, *RIM1-HA3*, and a control *RIM1* allele permitted equally high levels of *ime2-lacZ* expression and efficient sporulation; *RIM1-HA1* permitted slightly lower levels of *ime2-lacZ* expression and sporulation. A control *rim1* Δ 12 allele caused a 60-fold defect in *ime2-lacZ* expression and sporulation. Based upon these assays, the *RIM1-HA2* and *RIM1-HA3* alleles are completely functional and the *RIM1-HA1* allele is partially functional.

The *RIM1-HA2* protein product (Rim1-HA2p) was visualized on an immunoblot through reaction with anti-HA antibodies (Figure 3). In glucose-grown cells, Rim1-HA2p existed in two forms of apparent molecular masses 98 and 90 kD (lane 1). Both proteins were specified by *RIM1-HA2* because neither was detected in extracts of a *RIM1* strain (lane 5), which expressed no epitope-tagged product. In addition, both Rim1-HA1p and Rim1-HA3p were detected as two forms of 90 and 82 kD, as expected from presence of only a single epitope cassette (data not shown). In acetate-grown cells, only the 90-kD form of Rim1-HA2p was detectable (Figure 3, lane 6). Although the calculated Rim1-HA2p molecular mass is 82 kD, bacterially produced Rim1-HA2p has an apparent molecular mass of 98 kD (Figure 4, lane 3). Therefore, the 90-kD Rim1-HA2p form cannot be the *RIM1-HA2* primary translation product. (We note that the 98-kD Rim1-HA2p form migrates as a broad band or doublet; the leading edge comigrates with bacterial Rim1-HA2p.) It is unlikely that the 90-kD form of Rim1-HA2p is a nonspecific *in vitro* degradation product because (1) cell extracts were prepared by rapid boiling of whole cells, so the opportunity for *in vitro* proteolysis was minimized; (2) both Rim1-HA2p forms were observed in a protease-deficient *pep4* mutant (data not shown); (3) overexpression of Rim1-HA2p from a multi-copy *RIM1-HA2* plasmid or by fusion of *RIM1-HA2* to the *GAL1* promoter results in preferential accumulation of the 98-kD form, thus suggesting that production of the 90-kD form is a saturable reaction (data not shown); and (4) functional studies below argue that the 90-kD form is the active species *in vivo*. We conclude that Rim1p can exist in two forms whose relative levels respond to growth medium composition.

We considered the possibility that *RIM8*, *9*, and *13* might be required for Rim1p modification. We observed that *rim8-1*, *rim9-1*, and *rim13-1* strains accumulate only the 98-kD form of Rim1-HA2p (Figure 3, lanes 2–4 and 6–8), as do *rim9* Δ 2 and *rim9-10* strains (data not shown). Overall levels of Rim1-HA2p accumulation was unaffected by the *rim* mutations. Similarly, a *rim9-1* mutant accumulated only the 90-kD form of Rim1-HA1p, not the 82-kD form (data not shown). Therefore, *RIM8*, *9*, and *13* are required for production of the small form of Rim1p (the 90-kD Rim1-HA2p form) and

<i>RIM1</i> allele	Diagram	<i>RIM1</i> Function	
		<i>ime2-lacZ</i> Expression	Sporulation (%)
<i>RIM1-HA1</i>		76±9	21±1
<i>RIM1-HA2</i>		180±15	64±4
<i>RIM1-HA3</i>		177±34	78±7
<i>RIM1</i>		205±24	74±9
<i>rim1Δ</i>		3.2±0.3	1.3±1

for disappearance of large form of Rim1p (the 98-kD Rim1-HA2p form).

We considered a model in which the large form of Rim1p undergoes proteolytic cleavage to yield the small form. The cleavage would have to occur near the Rim1p C-terminus because we had observed both large (90 kD) and small (82 kD) forms of Rim1-HA1p, which has N-terminal HA epitopes. This model predicts that the 8-kD C-terminal Rim1p fragment resulting from cleavage should be detectable. We were unable to detect such a fragment from a Rim1p derivative with C-terminal HA epitope tags (at codon 613; data not shown). Detection

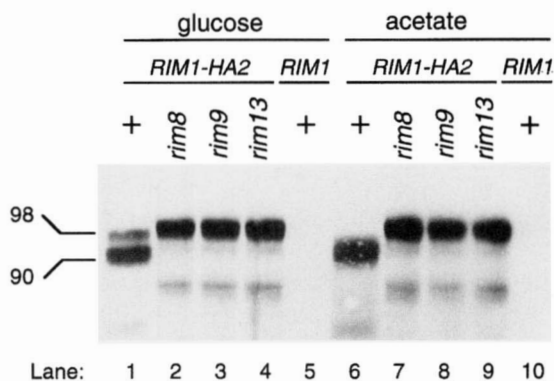


FIGURE 3.—Effects of *rim8*, *9*, and *13* mutations on Rim1-HA2p. Extracts of cells grown in glucose medium (lanes 1–5; YPD medium) or acetate medium (lanes 6–10; YPAC medium) were analyzed on an immunoblot with anti-HA antibodies. Strains were AMP1591 (*RIM1-HA2*; lanes 1 and 6), AMP1582 (*RIM1-HA2 rim8-1*; lanes 2 and 7), AMP1584 (*RIM1-HA2 rim9-1*; lanes 3 and 8), AMP1583 (*RIM1-HA2 rim13-1*; lanes 4 and 9), and AMP1606 (*RIM1*; lanes 5 and 10).

might have been compromised by instability or heterogeneity of the fragment; either problem might be overcome through fusion of a stable protein product to the Rim1p C-terminus. Therefore, we constructed a *RIM1-lacZ* gene that fuses β -galactosidase within the HA epitope at Rim1p codon 613 (Figure 5A). The fusion protein has a calculated molecular mass of 190 kD; the predicted proteolytic cleavage should yield a 130-kD C-terminal fragment. Two *RIM1-lacZ* products were detectable with anti- β -galactosidase antibodies, as revealed by comparison of *RIM1* and *RIM1-lacZ* strains (Figure 5B, lanes 1 and 2, respectively). The estimated sizes of the products corresponded closely to the predicted sizes. The model further predicts that only the 190-kD *RIM1-lacZ* product should be detectable in a *RIM1-lacZ rim9Δ* strain. As predicted, we could detect only the 190-kD product, and not the 130-kD product, in a *RIM1-lacZ rim9Δ* strain (Figure 5B, lane 3). These results indicate that proteolytic cleavage of the large Rim1p form yields the small form and a C-terminal fragment.

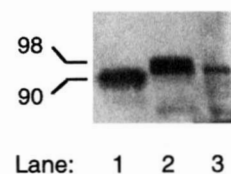


FIGURE 4.—Comparison of yeast and recombinant Rim1-HA2p. Extracts of YPAC-grown yeast strains AMP1591 (*RIM1-HA2*; lane 1) and AMP1601 (*rim9-10 RIM1-HA2*; lane 2) and an extract of *E. coli* strain BL21 expressing Rim1-HA2p (lane 3) were analyzed on an immunoblot with anti-HA antibodies.

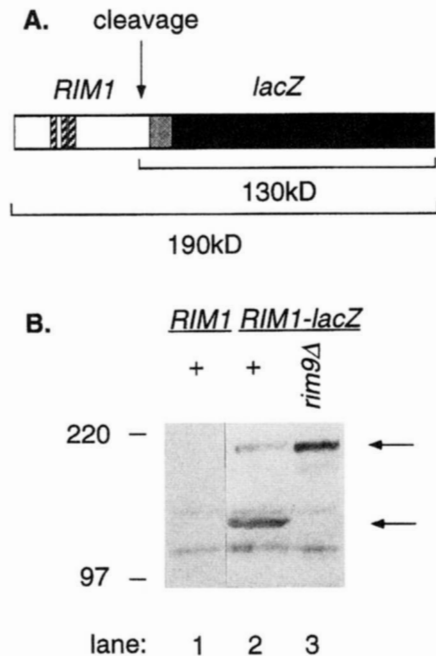


FIGURE 5.—Accumulation of *RIM1-lacZ* products. (A) Diagram of the *RIM1-lacZ* primary translation product. *RIM1* was fused to *lacZ* at codon 613; the fusion junction includes a portion of an HA epitope cassette (not diagrammed). The approximate site of expected proteolytic cleavage is indicated. (B) Detection of *RIM1-lacZ* products. Extracts of YPD-grown yeast strains AMP1606 (*RIM1 RIM9*, lane 1), AMP1686 (*RIM1-lacZ RIM9*, lane 2), and AMP1688 (*RIM1-lacZ rim9*) were analyzed on an immunoblot with anti- β -galactosidase antibodies. Positions of 220- and 97-kD size markers and of *RIM1-lacZ* products are indicated on the left and right, respectively.

Suppression of *rim* mutations by truncation of Rim1p: Observations reported above are consistent with the idea that Rim1p may be activated by removal of C-terminal residues, and that *RIM8*, *9*, and *13* are required for this proteolytic processing reaction. This model predicts that deletions that remove Rim1p C-terminal sequences may act as bypass suppressors of *rim8*, *9*, and *13* defects. Therefore, we looked among *RIM1* 3' deletion mutants for suppressors of *rim* mutations.

We first tested functional activity of plasmid-borne *RIM1* 3' deletion alleles by their ability to complement a *rim1* Δ mutation (Figure 6). Complementation was determined through two functional assays in a *rim1* Δ /*rim1* Δ *his3* Δ /*his3* Δ *ime1-HIS3*/*IME1 ime2-lacZ*/*IME2* strain. One assay relied upon the *ime1-HIS3* gene, for which the *RIM1*-dependent *IME1* promoter drives expression of the *HIS3* coding region. The strain is His⁻ due to lack of *RIM1* function (SU and MITCHELL 1993b), as confirmed by control complementation tests: a full-length *RIM1* plasmid (pSS179*RIM1*) conferred a His⁺ phenotype, whereas the vector (pRS314) did not. Deletions of *RIM1* to codon 485 permitted detectable function; two more extensive deletions abolished *RIM1* function. A second assay relied upon the *IME1*-depend-

ent *ime2-lacZ* gene, through which *IME1* expression (hence *RIM1* activity) may be assayed indirectly. This assay was carried out in sporulating cells, whereas *ime1-HIS3* expression assays were carried out in growing cells. The strain fails to express *ime2-lacZ*; the *RIM1* plasmid (pSS179*RIM1*) permits *ime2-lacZ* expression. Again, deletions of *RIM1* to codon 485 permitted function. Assessment of function through both *ime1-HIS3* and *ime2-lacZ* expression assays were in general agreement, though two partially functional plasmids (pKN32 and pKN30) were ranked differently in the two assays. We then introduced the plasmids into a *rim9* Δ 2/*rim9* Δ 2 *his3* Δ /*his3* Δ *ime1-HIS3*/*IME1 ime2-lacZ*/*IME2* strain to assay suppression (Figure 6). A low-copy *RIM9* plasmid (pSCRIM9) conferred a His⁺ phenotype and permitted *ime2-lacZ* expression; the vector (pRS314) did not. Intact *RIM1* and a deletion to amino acid residue 620 (pKN30) did not suppress *rim9* Δ 2, nor did the non-functional *RIM1* deletion derivatives (pKN35, pKN39). However, deletions ending between amino acid residues 539 and 485 (pKN36, pKN34, and pWL86) permitted strong suppression of *rim9* Δ 2: the *ime2-lacZ* reporter gene was expressed at 60% of the level observed with *rim1* Δ complementation by each plasmid, and at 40–80% of the level observed with *rim9* Δ complementation by pSCRIM9. Overexpression of *RIM1* from a high-copy plasmid (pMCRIM1) did not suppress *rim9* Δ 2 efficiently, though slight stimulation of *ime2-lacZ* expression was detected. These observations indicate that removal of the Rim1p C-terminus permits *IME1* promoter activity in the absence of *RIM9* function.

We extended these suppression studies with *RIM1-HA2-531*, a genomic *RIM1-HA2*-derived allele that has a 3' deletion to codon 531. Both *RIM1-HA2* and *RIM1-HA2-531* were crossed into *rim* mutant strains, and suppression was assayed by *ime2-lacZ* expression, growth at low temperature, colony morphology, and invasive growth. We observed that *RIM1-HA2-531* suppressed *rim8-1*, *rim9-10*, and *rim13-1* mutations, based upon all four assays (Table 2). These results support the hypothesis that Rim1p acts downstream of Rim8p, 9p, and 13p to promote all functions of this regulatory pathway.

The hypothesis that Rim1p is activated by C-terminal cleavage predicts that Rim1p C-terminal deletion derivatives should not undergo cleavage. We tested this prediction by comparison of Rim1-HA2p and Rim1-HA2-531p electrophoretic mobility (Figure 7). Rim1-HA2p existed as a 90-kD form in wild-type cells (lane 1) and as a 98-kD form in *rim8*, *9*, and *13* mutants (lanes 2–4). In contrast, Rim1-HA2-531p existed only as a 90-kD form in wild-type and *rim* mutant strains (lanes 5–8). We conclude that the Rim1p C-terminus includes sequences required for *RIM8*, *9*, and *13*-dependent proteolytic cleavage.

Effect of external pH on Rim1p: Observations above suggested that external glucose may promote accumula-










	<i>rim1</i> Complementation		<i>rim9</i> Suppression		Zinc Finger Regions	Acidic Region
	<i>ime1-HIS3</i>	<i>ime2-lacZ</i>	<i>ime1-HIS3</i>	<i>ime2-lacZ</i>		
pKN39	-	4	-	3		391
pKN35	-	3	-	4		473
pKN36	+	209	+/-	143		485
pWL86	+	131	+	81		531
pKN34	+	217	+	160		539
pKN32	+/-	56	+/-	25		559
pKN30	+/=	118	-	3		620
pSS179RIM1	+	148	-	2		628
pMC RIM1	+	224	-	13		628
pRS314	-	6	-	5		
pSCRIM9	-	7	+	202		

FIGURE 6. — Activity of truncated Rim1p derivatives. Low-copy *RIM1* 3' deletion plasmids were transformed into strains AMP1578 (a/α *rim1* Δ 5/*rim1* Δ 5 *ime1-HIS3/IME1* *IME2::ime2-lacZ/IME2*) and AMP1592 (a/α *rim9* Δ 2/*rim9* Δ 2 *ime1-HIS3/IME1* *IME2::ime2-lacZ/IME2*) to test for complementation and suppression, respectively. *RIM1* 3' deletion endpoints lay at the codons indicated in the right column. Plasmids pSS179RIM1 (low-copy) and pMCRIM1 (high copy) specify full-length *RIM1*, which terminates after codon 628; plasmid pRS314 is the low-copy plasmid vector with no *RIM1* insert. Plasmid pSCRIM9 is a low-copy *RIM9* plasmid (pWL51). Complementation and suppression were assayed by expression of *ime1-HIS3*, as determined by growth on medium lacking histidine, and of *ime2-lacZ*, as determined by β -galactosidase assays. Standard deviations for triplicate β -galactosidase assays were within 20% of the mean, except for assays with plasmid pKN32 in strain AMP1592, which yielded a standard deviation of 50% of the mean.

tion of the large form of Rim1p (Figure 1). In support of this hypothesis, we observed that growth in presence of unusually high glucose concentrations (5, 10, or 20%) led to increased accumulation of the 98-kD Rim1-HA2p form and had little effect on the 90-kD form (data not shown). The report by OREJAS *et al.* (1995) that *Aspergillus* PacC processing responds to external pH led us to wonder whether high glucose concentrations might affect pH of the growth medium. We observed that glucose did not affect the initial pH of the culture (pH 6.5 for YPD medium), but that increasing glucose concentrations caused exponential cultures to have a more acidic pH (*e.g.*, pH 6.0 for YPD medium with 2% glucose). In contrast, exponential acetate cul-

tures had a neutral pH (pH 7.0 for YPac with 2% potassium acetate). Thus our findings were also consistent with the hypothesis that external acidity promotes accumulation of the large form of Rim1p. To determine whether pH or carbon source was responsible for effects on Rim1p, we examined Rim1-HA2p in cells grown in buffered glucose and acetate media (Figure 8). Regardless of carbon source, acidic pH caused accumulation of both 98- and 90-kD Rim1-HA2p forms (lanes 1 and 3); neutral or alkaline pH caused accumulation of only the 90-kD Rim1-HA2p form (lanes 2 and 4). We also observed that a *rim9-10* mutant accumulated only the 98-kD Rim1-HA2p form at either pH 4.4 or 8.0 in glucose medium (data not shown). These results indicate

TABLE 2
Suppression of *rim8*, *9*, and *13* mutations by the *RIM1-HA2-531* 3' deletion mutation

Strain	Relevant genotype	Colony morphology ^a	Invasive growth ^b	<i>ime2-lacZ</i> expression ^c	17° growth
AMP1602	<i>rim8 RIM1-HA2</i>	Smooth	—	1	—
AMP1597	<i>rim8 RIM1-HA2-531</i>	Rough	+	95	+
AMP1601	<i>rim9 RIM1-HA2</i>	Smooth	—	1	—
AMP1598	<i>rim9 RIM1-HA2-531</i>	Rough	+	80	+
AMP1603	<i>rim13 RIM1-HA2</i>	Smooth	—	1	—
AMP1599	<i>rim13 RIM1-HA2-531</i>	Rough	+	55	+
AMP1604	<i>RIM1-HA2</i>	Rough	+	100	+
AMP1600	<i>RIM1-HA2-531</i>	Rough	+	135	+

^a Colony morphology was scored by visual inspection.

^b Invasive growth was scored by adherence of cells to a YPD plate after washing the plate surface.

^c *ime2-lacZ* expression was measured after incubation for 8 hr in sporulation medium. Values in Miller units are the means of triplicate determinations; SD, \pm 15%.

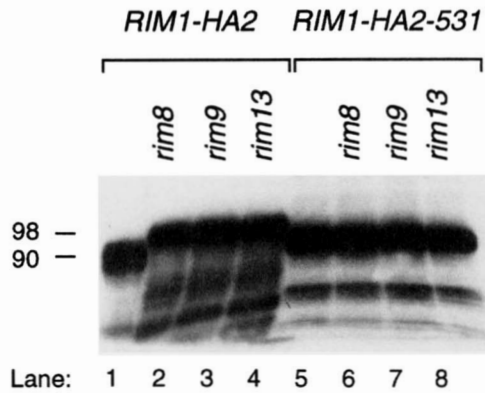


FIGURE 7.—Accumulation of Rim1-HA2p and Rim1-HA2-531p in *rim8*, *9*, and *13* mutants. Extracts of *RIM1-HA2* strains (lanes 1–4) and *RIM1-HA2-531* strains (lanes 5–8) were compared on an immunoblot. Strains carried additional mutations *rim8-1* (lanes 2 and 6), *rim9-10* (lanes 3 and 7), or *rim13-1* (lanes 4 and 8), and are listed in Table 2.

that accumulation of the large form of Rim1p is favored by external acidity, and that the effects of carbon source are an indirect consequence of pH changes from metabolism.

DISCUSSION

Rim1p, 8p, 9p, and 13p were proposed to have a close functional relationship because of shared mutant phenotypes and properties of double mutants (SU and MITCHELL 1993a). These studies were consistent with action of the *RIM* gene products either in a linear pathway or in a protein complex. Our analysis of Rim1p supports and extends that proposal. We have shown that *rim8*, *9*, and *13* mutations affect Rim1p qualitatively, as detected by a change in Rim1p electrophoretic mobility. This observation provides a more direct biochemical link between the *RIM* gene products. It also suggests that Rim1p acts downstream of Rim8p, 9p, and 13p in a linear pathway.

Structural and functional observations together argue that Rim1p may be activated by C-terminal proteolytic cleavage. The two forms of Rim1p differ by an

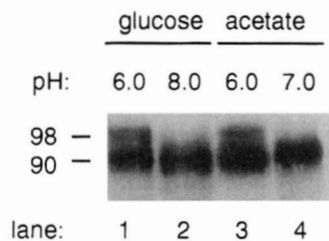


FIGURE 8.—Effect of external pH on Rim1-HA2p processing. Rim1-HA2p was detected on an immunoblot after growth of strain AMP1591 (*RIM1-HA2*) in glucose medium (YPD) buffered at pH 5.5 (lane 1) or pH 8.0 (lane 2), or in acetate medium (YPAc) buffered at pH 6.0 (lane 3) or pH 7.0 (lane 4).

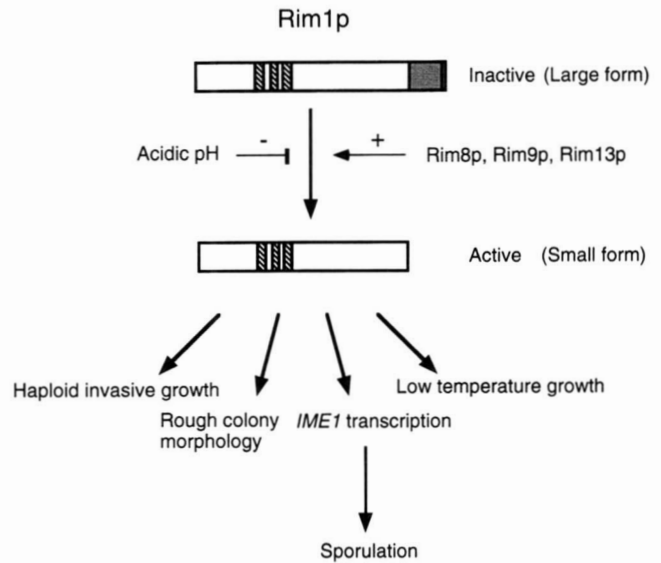


FIGURE 9.—Model for relationships among Rim1p, 8p, 9p, 13p, and external pH. Rim1p is activated by a proposed C-terminal proteolytic cleavage, which depends upon Rim8p, 9p, and 13p and is inhibited by acidic external pH. Active Rim1p permits haploid invasive growth, rough colony morphology, *IME1* expression (leading to *IME2* expression and sporulation), and growth at low temperatures. Although the diagram suggests that external pH acts independently of Rim8p, 9p, and 13p, it is also possible that acidic external pH inhibits Rim1p processing through inhibition of Rim8p, 9p, or 13p expression or activity.

apparent mass of 8 kD, which corresponds to ~70 amino acid residues. The small form of Rim1p, which is predominant in wild-type strains, has greater electrophoretic mobility than recombinant Rim1p expressed in *E. coli*. This observation suggests that the small Rim1p form might be produced through proteolytic cleavage of the large Rim1p form. Two forms of a Rim1p derivative with an N-terminal HA epitope (Rim1-HA1p) are detectable with anti-HA antibodies, so proteolytic cleavage would have to occur near the Rim1p C-terminus. This idea is consistent with the observation that *RIM1-lacZ* produces a 130-kD form of β -galactosidase. It is also supported by the finding that Rim1-531p, which lacks the C-terminal 97 residues, apparently exists in only one form. In *rim8*, *9*, and *13* mutants, only the large Rim1p form accumulates; because these mutants have the same phenotype as a *rim1* Δ null mutant, we infer that the large Rim1p form is inactive. Suppression of *rim8*, *9*, and *13* mutations by expression of Rim1-531p indicates that removal of Rim1p C-terminal residues is sufficient to produce a biologically active protein in these mutants. We propose a simple model to summarize these results (Figure 9). Rim1p is synthesized as a precursor that is activated by proteolytic removal of a C-terminal segment (~70 amino acid residues); proteolytic activation requires Rim8p, 9p, and 13p.

The ability of *RIM1-531* and other altered *RIM1* al-

les to suppress *rim8*, *9*, and *13* mutant phenotypes lends strong support to the idea that Rim1p acts downstream of Rim8p, 9p, and 13p. This argument is most compelling for Rim9p because true *rim9* null mutations are suppressed. In principle, overexpression of *RIM1* might be expected to suppress the other *rim* mutations. Indeed, the composition of the Rim1p C-terminus resembles that of destabilizing PEST sequences (ROGERS *et al.* 1986; RECHSTEINER and ROGERS 1996), so suppression by *RIM1-531* might have resulted from elevated Rim1-531p accumulation. However, neither a high copy *RIM1* plasmid nor a *GAL1-RIM1* fusion gene can suppress *rim8*, *9*, and *13* mutations efficiently, though they do complement a *rim1* mutation and result in substantial hyperaccumulation of the large Rim1p form (W. LI and A. P. MITCHELL, unpublished results). We also observed that Rim1p and Rim1-531p accumulate to comparable levels. Therefore, suppression results from a qualitative change in Rim1p, not an increase in Rim1p accumulation.

Although accumulation of the large Rim1p form is greatest in acidic media, we have not found strong evidence that Rim1p transmits a pH-dependent signal. Two Rim1p-dependent processes, invasive growth and *ime2-lacZ* expression, are inhibited in acidic media (W. LI and A. P. MITCHELL, unpublished observations). These observations are consistent with the idea that functional Rim1p activity is diminished in acidic media. However, acid inhibition of invasive growth and *ime2-lacZ* expression are not relieved in *RIM1-531* strains. This observation indicates that acid inhibition of these processes is not exerted solely by inhibition of Rim1p processing. In fact, cells grown in acidic media accumulate the same active (small) Rim1p, so they may retain substantial Rim1p functional activity.

The deduced structures of Rim1p and Rim9p are consistent with the idea that they act in a linear pathway. Rim1p has three zinc fingers, so a simple possibility is that Rim1p acts as a transcription factor (SU and MITCHELL 1993b). Although Rim1p is formally a positive regulator of *IME1*, we do not know whether it may act more directly as a transcriptional activator or repressor when bound to DNA. Rim9p has four hydrophobic segments (Figure 10). The three internal segments are potential transmembrane domains; the N-terminal segment may function either as a transmembrane domain or signal sequence. Membrane-association of Rim9p is consistent with its acting upstream of a transcription factor in a signal transduction pathway. Rim9p may function as transmembrane receptor that responds to an extracellular, intracompartamental, or intramembrane signal. A second possibility is that Rim9p acts more directly as a subunit of a membrane-bound protease; such an activity is required for proteolytic activation of *Bacillus* σ^E (HOFMEISTER *et al.* 1995).

Three observations indicate that similarities of Rim1p

A.

```

1  MVSMIHIVVFLLAITTMFEILPLITVPVTKYLSLSSFFNHHYYG
44  LFGWCVFGQNQLMCTKMKIGYDSTDVDSSGHVLTLPNSNK
77  VVVSNLLVVHPISLAFTGTLILLAVIIMVTPLGDSPPELLFT
120 ALFSLPTFMLCLLCLFLVDILLFISKLDWPGWLMMLAATISVAL
163 CCSMLVVMFRVVSVKKYESQQSIAHACSMIEQYSISDIYQSK
206 QNGNSSEYEVAPTHDSLIAPEVTYRGFIE

```

B.

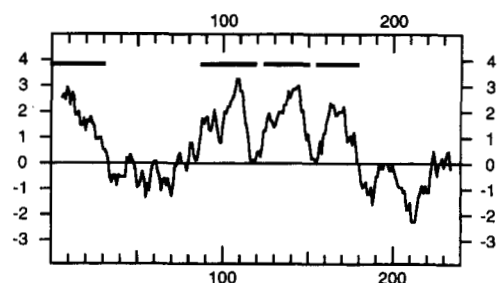


FIGURE 10.—Structural features of Rim9p. (A) The deduced Rim9p amino acid sequence, with hydrophobic segments underlined. (B) Kyte-Doolittle hydropathy plot of Rim9p.

to *Aspergillus* PacC extend beyond general structural features. First, Rim1p and PacC both accumulate in two forms, though the size difference between PacC forms (400 residues; OREJAS *et al.* 1995) is much greater than between Rim1p forms (70 residues). Second, the small forms of both Rim1p and PacC appear to be the active forms (this study; OREJAS *et al.* 1995; TILBURN *et al.* 1995). Third, accumulation of the large forms of both Rim1p and PacC is favored in acidic medium (this study and OREJAS *et al.* 1995). An interesting possibility is that Rim8p, 9p, and 13p may be homologous to some of the *Aspergillus pal* gene products, which govern activation of PacC (OREJAS *et al.* 1995).

We are grateful to HERB ARST for drawing our attention to PacC. We thank members of this laboratory, past and present, for many helpful discussions. This work was supported by a grant from the National Institutes of Health (GM-39531) to A.P.M.

LITERATURE CITED

- ALANI, E., L. CAO and N. KLECKNER, 1987 A method for gene disruption that allows repeated use of *URA3* selection in the construction of multiply disrupted yeast strains. *Genetics* **116**: 541–545.
- BLACKETER, M. J., C. M. KOEHLER, S. G. COATS, A. M. MYERS and P. MADAULE, 1993 Regulation of dimorphism in *Saccharomyces cerevisiae*: involvement of the novel protein kinase homolog Elm1p and protein phosphatase 2A. *Mol Cell Biol.* **13**: 5567–5581.
- BOWDISH, K. S., H. E. YUAN and A. P. MITCHELL, 1994 Analysis of RIM11, a yeast protein kinase that phosphorylates the meiotic activator IME1. *Mol Cell Biol.* **14**: 7909–7919.
- COVITZ, P. A., I. HERSKOWITZ and A. P. MITCHELL, 1991 The yeast *RME1* gene encodes a putative zinc finger protein that is directly repressed by $\alpha 1-\alpha 2$. *Genes Dev.* **5**: 1982–1989.
- DAILEY, D., G. L. SCHIEVEN, M. Y. LIM, H. MARQUARDT, T. GILMORE *et al.*, 1990 Novel yeast protein kinase (*YPK1* gene product) is a 40-kilodalton phosphotyrosyl protein associated with protein tyrosine kinase activity. *Mol. Cell Biol.* **10**: 6244–6256.
- GIMENO, C. J., P. O. LJUNGDAHL, C. A. STYLES and G. R. FINK, 1992

- Unipolar cell divisions in the yeast *S. cerevisiae* lead to filamentous growth: regulation by starvation and RAS. *Cell* **68**: 1077–1090.
- HOFMEISTER, A. E., A. LONDOND-VALLEJO, E. HARRY, P. STRAGIER and R. LOSICK, 1995 Extracellular signal protein triggering the proteolytic activation of a developmental transcription factor in *B. subtilis*. *Cell* **83**: 219–226.
- KAISER, C., S. MICHAELIS and A. MITCHELL, 1994 *Methods in Yeast Genetics*. Cold Spring Harbor Laboratory Press, Cold Spring Harbor, NY.
- KANE, S., and R. ROTH, 1974 Carbohydrate metabolism during ascospore development in yeast. *J. Bacteriol.* **118**: 8–14.
- MILLER, J. J., 1989 Sporulation in *Saccharomyces cerevisiae*, pp. 491–529 in *The Yeasts*, edited by A. H. ROSE and J. S. HARRISON. Academic Press, San Diego.
- MITCHELL, A. P., 1994 Control of meiotic gene expression in *Saccharomyces cerevisiae*. *Microbiol. Rev.* **58**: 56–70.
- MYERS, A. M., A. TZAGALOFF, D. M. KINNEY and C. LUSTY, 1986 Yeast shuttle and integrative cloning vectors with multiple cloning sites suitable for construction of lacZ fusions. *Gene* **45**: 299–310.
- NEIGEBORN, L., and A. P. MITCHELL, 1991 The yeast *MCK1* gene encodes a protein kinase homolog that activates early meiotic gene expression. *Genes Dev.* **5**: 533–548.
- OREJAS, M., E. A. ESPESO, J. TILBURN, S. SARKAR, H. N. ARST JR. *et al.*, 1995 Activation of the *Aspergillus* PacC transcription factor in response to alkaline ambient pH requires proteolysis of the carboxy-terminal moiety. *Genes Dev.* **9**: 1622–1632.
- PAYNE, M. J., P. M. FINNEGAN, P. M. SMOOKER and H. B. LUKINS, 1993 Characterization of a second nuclear gene, *AEP1*, required for expression of the *OLH1* gene in *Saccharomyces cerevisiae*. *Curr. Genet.* **24**: 126–135.
- RECHSTEINER, M., and S. W. ROGERS, 1996 PEST sequences and regulation by proteolysis. *Trends Biol. Sci.* **21**: 267–271.
- ROBERTS, R. L., and G. R. FINK, 1995 Elements of a single MAP kinase cascade in *Saccharomyces cerevisiae* mediate two developmental programs in the same cell type: mating and invasive growth. *Genes Dev.* **8**: 2974–2985.
- ROGERS, S., R. WELLS and M. RECHSTEINER, 1986 Amino acid sequences common to rapidly degraded proteins: the PEST hypothesis. *Science* **234**: 364–368.
- ROSE, M. D., P. NOVICK, J. H. THOMAS, D. BOTSTEIN and G. R. FINK, 1987 A *Saccharomyces cerevisiae* genomic plasmid bank based on a centromere-containing shuttle vector. *Gene* **60**: 237–243.
- SHAH, J. C., and M. J. CLANCY, 1992 *IME4*, a gene that mediates *MAT* and nutritional control of meiosis in *Saccharomyces cerevisiae*. *Mol. Cell Biol.* **12**: 1078–1086.
- SHERO, J. H., and P. HIETER, 1991 A suppressor of a centromere DNA mutation encodes a putative protein kinase (*MCK1*). *Genes Dev.* **5**: 549–560.
- SIKORSKI, R. S., and P. HIETER, 1989 A system of shuttle vectors and yeast host strains designed for efficient manipulation of DNA in *Saccharomyces cerevisiae*. *Genetics* **122**: 19–27.
- SMITH, H. E., and A. P. MITCHELL, 1989 A transcriptional cascade governs entry into meiosis in yeast. *Mol. Cell Biol.* **9**: 2142–2152.
- STUDIER, F. W., A. H. ROSENBERG, J. J. DUNN and J. W. DUBENDORFF, 1990 Use of T7 RNA polymerase to direct expression of cloned genes. *Methods Enzymol.* **185**: 60–89.
- SU, S. S. Y., and A. P. MITCHELL, 1993a Identification of functionally related genes that stimulate early meiotic gene expression in yeast. *Genetics* **133**: 67–77.
- SU, S. S. Y., and A. P. MITCHELL, 1993b Molecular analysis of the yeast meiotic regulatory gene *RIM1*. *Nucleic Acids Res.* **21**: 3789–3797.
- TILBURN, J., S. SARKAR, D. A. WIDDICK, E. A. ESPESO, M. OREJAS *et al.*, 1995 The *Aspergillus* PacC zinc-finger transcription factor mediates regulation of both acid- and alkaline-expressed genes by ambient pH. *EMBO J.* **14**: 779–790.
- TYERS, M., G. TOKIWA and B. FUTCHER, 1993 Comparison of the *Saccharomyces cerevisiae* G1 cyclins: Cln3 may be an upstream activator of Cln1, Cln2, and other cyclins. *EMBO J.* **12**: 1955–1968.
- ZIAJA, K., G. MICHAELIS and T. LISOWSKY, 1993 Nuclear control of messenger RNA expression for mitochondrial ATPase subunit 9 in a new yeast mutant. *J. Mol. Biol.* **229**: 909–916.

Communicating editor: F. WINSTON